A STUDY OF '1'1 IE LINE PROFILE OF H LYMAN-β FROM DISSOCIATIVE EXCITATION 01'"1$

JOSEPH M. AJELLO
SYED M. AHMED
XIANMING LIU

JET PROPULSION LABORATORY
CALIFORNIA INSTITUTE OF TECHNOLOGY
PASADENA, CALIFORNIA 91109

SUBMITTED '1'0 :
PHYSICAL REVIEW A

JULY 15, 1995

ABSTRACT

A high-resolu ion ultraviolet (uv) spectrometer was employed for the first measurement of the H Lyman-β (}1 Lβ) emission Doppler line profile a t 1025.7 Å from dissociative excitation of H_2 by electron impact. Analysis of the (ice.onvolvcci line profile reveals the. existence of a narrow central peak, less than 30 mÅ full-width-h alf-maximu m (FWHM) and a broad pedestal base shout 260 mÅ FWHM. Analysis of the red wing of the line profile is complicated by a group of Werner and Lyman rotational lines 160 to 2 2() mÅ from line center. Analysis of the blue wing of the line profile gives th c kinetic energy distribution. '1'here arc two main kinetic energy components to the H(3p) distribution: 1) a slow distribution with a peak value near O CV from singly excited states and 2) a fast distribution with peak contribution near 7 eV from doubly excited states. Using two di fferent techniques, the absolute cross section of 11 Lβ is found 10 bc 3.28 ± 0.80 x 10^{-19} cm^2 a t 100 eV c ectron impact energy. The exper mental cross section and line profile results can be compared to previous studies of Hα (6563.7 Å) for principal quantum number n=3 and of Lα (121 5.7 Å) for n=2.

PACS CLASSIFICATION: 34.80.Gs (ELECTRON SCATTERING -MOLECULAR DISSOCIATION), 33.50Dq (Mel .ECULAR SPECTRA - FLUORESCENCE

INTRODUCTION

For many years high resolution studies in the visible region of the spectrum have been carried out on the Balmer series {principal quantum number, n=3, 4 and 5 excited states) of H produced by dissociative excitation of H_2 upon electron impact. For each principal quantum number, two major sets of kinetic energy distributions were found, corresponding to the "slow" and "fast" distributions with typical kinetic energies of near 0 eV and 4-10 eV, respectively. The principal architects of these measurements were Ogawa and co-workers.[1-3] They have carefully shown that the two kinetic energy distributions reflect effects of dissociation from singly excited bound states (slow component) and from repulsive doubly excited states (fast component). Recently, we have begun high resolution studies of the Lyman series of H from dissociative excitation of H_2,[4,5] utilizing a high resolution 3-meter vacuum ultraviolet (vuv) spectrometer with a resolving power of greater than **50000.**[6] We reported the first measurement of the H Lyman-α (H Lα) emission Doppler profile from dissociative excitation of H_2 by electron impact. Analysis of the deconvolved line profile revealed the existence of a narrow central peak of 40 ± 4 mÅ FWHM and a broad pedestal base about 240 mÅ wide FWHM. Slow H(2p) atoms with peak energy near 80 meV produce the peak profile, which is nearly ndependent of impact energy. The wings of H Lα arise from dissociative excitation of a series of doubly excited Q_1 and Q_2 states, which define. the core orbitals. The energy distribution of the fast atoms **shows** a peak at about **4** eV. in this work we extend the measurements to he 3p state and compare our results to line profile studies of Hα. The Hα inc profile shows a characteristic narrow central peak (-300 mÅ FWHM) from the slow component and a broad wing (-1.8 Å FWH M) from the fast Component in the optical region. Since the Doppler displacement is proportional to wavelength, six times narrower line profiles can b c expected in the vacuum ultraviolet (vuv) spectral region for the L ym a n series.

1 is also a goa of this study to directly measure the absolute cross section for H Lβ at 100 Cv for completely modeling the H_2 vacuum ultraviolet spectrum (vuv) for both calibration and astronomy purposes. Once before. in 1984 wc have applied published Hα absolute cross section results[7] to a low resolution H_2 Vuv spectrum from our laboratory t o determine the absolute H Lβ absolute cross section. ~

The most important application of the Lyman series line profiles is the opportunity to study and distinguish the emission spectrum of hydrogen from its molecular and atomic orms. The advent of h i g h resolution spacecraft such as the Hubble Space Telescope, equipped with the Goddard High Resolution Spectrograph and the planned astrophysical extreme ultraviolet observatories have lead to the measurement of the H $L\alpha$ line profile in both the auroral zones and the day glow. H $L\alpha$ line profile wings extending to ± 1 Å have been measured in the aurora by HST and line core widths of greater than 140 mÅ have been observed by IUE.[9,10] The primary cause of the dayglow is resonant scattering of solar emission with a broad line profile from multiple scattering. The main cause of the aurora is primary particle bombardment by electrons, protons and heavier ions followed by secondary electron excitation of the Lyman series. The large amount of Lyman and Werner band emission ensures that dissociative excitation of H_2 is an important process.

EXPERIMENTAL

The experimental system has been described by Liu et al.[6] in brief, the experimental system consists of a high-resolution 3-meter uv spectrometer in tandem with an electron impact collision chamber. For the H $L\beta$ line profile, a resolving power of 27,000 is achieved by operating the spectrometer in second order. The H $L\alpha$ line profile has been previously reported[4,5] **and** was measured in third order at a resolving power of 50,()()0. ' 'he line shapes were measured with experimental conditions that ensure 1 nearity of signal with electron beam current and background gas pressure. in this study the line profile spectra were measured in the crossed beam mode; and the one. low resolution H Lβ excitation function was obtained in the static gas mode. The operating conditions for the collision chamber included an electron beam current of 130 μA and an H_2 gas pressure of 2.3 x 10'4 torr. The electron -impact -induced -fluorescence line profiles of H Lα and H Lβ at 100 CV impact energy are shown in Fig. 1, along with the instrumental slit function of the spectrometer in second order. It is found that the H .β line profile has a red wing that is blended b y three moderately strong Lyman (L) and Werner (W) rotational lines, detailed in 'J'able 1 among other rotational lines in the neigborhood of the red wing of I I Lβ. One of the three strong incs is the L 1(6,0)Q resonance line, lying furthest from H Lβ line center. The closest, the W 1 (5,3)Q rotational line lies 163 mÅ from H Lβ line. center. W c estimate the extent of the red wing by reflecting hc blue wing about line center, It is shown as a dashed line in Fig. 1. The major wing of the H 1$ line profile extends 150 mÅ from line center. A very weak secondary pedestal wing extends to 175 mÅ from line center. By comparison the H Lα wing extends 1 40 mÅ (reported FWHM =240 mÅ) from line center.[4,5] The Doppler wavelength shift is proportional to the rest wavelength. Much greater kinetic energies are released during n=3p dissociation than for n=2 › (Dissociation to account for the broader H Lβ line profile.

The weak signal from H Lβ in third order prompted the second order study. Yet note the line core FWHM is nearly (4o mÅ vs 38 mÅ) at the limit of the second order slit function. It is slightly narrower than the third order line core profile from H Lα even though the H Lα slit function was a narrow 24 mÅ that is indicated in Fig. 1. For this reason it will not be possible 10 accurately determine the slow atom distribution function as w c were able to do for H Lα.[4,5]

11 Lβ CROSS SECTION AT 100eV

The first step in our comparative study of 11 Lα and H Lβ was to measure the absolute cross section of H Lβ at 100 cV. We can find the cross section by two methods. One method relies on the absolute cross section of H Lα al 10(cV, together with a relative calibration of H Lα and H Lβ line intensities, and the other method uses the absolute cross sections of the three major L& W features in the red wing of H Lβ.

For the first method, the cross section of H Lα has been measured to be 7.3 x 10^{-18} cm^2 at 100 eV.[11] The relative calibration in the vuv at 100 eV, using the H_2 "many line" spectrum, has been described in fine structure.[6,11] The two step process involved: 1) measuring the H Lβ to H Lα intensity ratio at 100 eV and 2) determining the relative calibration between 1025 Å and 121.6 Å. The wavelength calibration was performed in second order using the synthetic vuv line intensities of Liu et al.[6] convolved to the same resolution as the experimental low resolution spectrum. Approximately sixteen continuous 25 Å wide spectral regions resolution provided a smooth second order calibration curve between 900 and 1300 Å. A typical first order FUV calibration curve is shown in Liu et al." By applying this first method, the ratio of cross sections was determined to be Q(H Lβ)/Q(H Lα) = 0.0412 at 100 eV. Q(H Lβ) is 3.01 $\pm$ 0.75 x 10^{-19} cm^2.

The second method gave an independent evaluation of the cross section. It is also a method that is free of instrument calibration. We have recently measured for the first time the L & W fine structure direct cross section energy dependence from 0 - 1 keV (Liu et al., unpublished). Using the oscillator strengths of Abgrall et al.[12-14], we are able to place on an absolute scale the cross section for every rotational line at 100 eV. The three strong L & W rotational lines found in the red wing of the H Lβ line are shown in Table 1, along with corresponding intensities. The L (6,0)1^{1}L rotational line required a 40% correction for optical depth at the measurement pressure of 2.3 x 10-4 torr and the path length of foreground gas of 11.05 cm. The fractional L & W area of the total blended Lβ + L & W feature in Fig.1 is 42.4%. The ratio of Q(Lβ)/Q(L&W) is 1.36. At 100 eV, we find the cross section of H Lβ to be 3.43 ± 0.8S x 10^{-19} cm^{2}. The average cross section of H Lβ at 100 eV based on these two methods is 3.22 ± 0.80 x 10^{-19} cm^{2}. The total cross section of the blended feature in Fig.1 is 5.69 ± 1.40 x 10^{-19} cm^{2}

KINETIC ENERGY DISTRIBUTION OF FAST PRODUCTS

The determination of the kinetic energy distribution of the products is a two-step process that we have described in the previous paper on H Lα.[4,5] The resolution of the experiment is not sufficient to recover the slow distribution of H(3p) atoms. However, the width of the wings is broad with respect to the instrument slit function. On this basis it should be possible to locate the peak of the kinetic energy distribution function of fast H(3p) and estimate the shape of the distribution function. The measured line profile is the convolution of the true line profile and the instrumental slit function. Expressed mathematically the measured line profile, $I(\lambda)$, is given by the convolution integral

$$I(\lambda)= \int T(\lambda') A(\lambda - \lambda')d \lambda', \quad (1)$$

where $T(\lambda')$ is the true line profile at wavelength λ' and $A(\lambda - \lambda')$ is the instrumental response function. In the transform domain the convolution becomes a simple product,

$$I_T(s)= T_T(s) A_T(s), \quad (2)$$

where I_T, T_T, and A_T are the FFT of I, T and A, respectively and s is measured in inverse wavelength. Optimal Wiener filtering of the measured signal, I, was performed, since it includes a small noise component.[15] Signal-to-noise ratio (S/N) is greater than 40 for all line profiles. The FFT of T is given by,

$$T_T(s)= I_T(s) F_T(s)/ A_T (s) , \quad (3)$$

where $F(\lambda)$ is the optimal filter. We selected a $cosine^{40}(s)$ to remove high frequency noise from the ratio of I_T/A_T. We show in Fig. 2 the inverse FFT (FFT^{-1}) of $T_T(s)$ for the 100 eV line profiles of H $L\alpha$ and H $L\beta$ compared to the wavelength scaled $H\alpha$ results of Freund et al.[16] and Higo et al.[2] The $L\beta$ feature arises from a single multiplet corresponding to the transition 1s-3p. However the $H\alpha$ feature consists of three multiplets from the transitions 2s-3p, 2p-3s and 2p-3d. Only the first $H\alpha$ mutiplet (2s-3p) shares the Same upper level. For that Hα multiplet the line profile would be identical to Lβ when scaled in wavelength by the factor 1025.7Å /6563.7Å, according to the Doppler principle. In the comparison in Fig. 2, we have assumed that all three multiples produce the same line profile. This is plausible since their 3ℓ dissociation asymptotes are degenerate.

The first interpretation from Fig. 2 comes from a comparison of the 100 eV line profiles of H Lα and H Lβ. The wings of f Lβ line profile are broader and more intense than H Lα. The FWHM of H Lα is 240 mÅ while the H Lβ line profile has a FWHM of 260 mÅ. The ratio of the two FWHM (Lβ/Lα) is a modest 1.08. This ratio can be used to find the ratio of the average kinetic energy for fast H(3p) and H(2p) atoms. The ratio is made larger by an additional factor of 1.41 when converting the Doppler shifts to an equivalent translational energy. More details on the energy dependence of the distribution are discussed below. As described earlier, we were only able to measure an unblended line profile for the blue wing of H Lβ. We have assumed the red wing is identical. Since the Hα line is slightly asymmetric, the same can be expected to be true of H Lβ. The comparison of the H Lβ line profile with the two published Hα line profiles is in quite good agreement with the results of Higo et al.[2] and verified recently by Ogawa et al.3 The comparison with Freund et al.[16] is quite poor. Those authors have pointed out that their Hα line profiles were flawed by spectrometer aberrations. Note the Hα line profile of Higo et al.[2] and the Lβ line profile indicate the appearance of a weak secondary wing extending to nearly **200** mÅ from Lβ line center. The initial indication from our data is that the line core of H Lα is broader than for H Lβ. in Fig. 1 at the lower resolution afforded by second order for H Lβ we find a narrower line than for H Lα. This result can be attributed to the energy scale relating to the processes for production of slow H(2p) atoms from direct excitation, cascade and predissociation, particularly the latter.[4,5,17,18] We place an upper limit of 30 mÅ on the FWHM of H Lβ compared to our previously reported value of 40 mÅ for H Lα.

For the 100 eV line profile The kinetic energy distribution of the fragments, P(E), is given by

$$P(E)= k(dT/d\lambda) \quad , \qquad (4)$$

where k is a multiplicative constant .19 With this approach, the 100 eV electron impact line profiles for H Lα and H Lβ in Fig. 2 were differentiated. The combined kinetic energy distributions of the fast and slow H(2p) and H(3p) fragments are shown in Fig. 3 for the blue wing of H Lα and H Lβ of Fig. 3. The results for the H(3p) atom distribution show a peak kinetic energy at 7 eV compared to the H(2p) peak near 4 eV. The high end of the distribution releases H-atoms with 10 eV kinet c energy. The low end of the distribution begins at about 1 eV. We have previously shown that th c H(2p) distribution changes with electron impact energy. A comparison of the results for H(3p) at 100 CV with those of Ogawa and co-workers is excellent. For example, their first measurement[1] of H(3ℓ) kinetic energy distribution from Hα line profile studies showed two kinds of kinetic energy distributions, an average kinetic energ y of 7 eV associated with the fast group and an average kinetic energy of 0.3 eV attributed to the slow group. More detailed analysis of the Balmer series by Higo et al.[2] followed. They measured the line profiles for Hα, Hβ and Hγ. At an electron impact energy of 100 **Cv,** the ranslational energy distributions had a fast peak a t 7-8 eV and a slow)eak at -O eV.

The high kinetic energy fragments result from dissociation through a series of repulsive curves which involve doubly excited electron orbitals. These doub y excited stales have been described by Guberman.[20] The Q_1 Rydbe g ser es of states consist of a $2p\sigma_u$ core orbital plus excited states of u symmetry. These repulsive states converge to the $^2\Sigma_u^+$ of H_2^+. The Q_2 Rydbe g series of states consist of a $2p\pi_u$ core orbits] plus excited slates. These repulsive states converge to the $^2\Pi_u$ of H_2^+. At 100 eV mpact energy, both the Q_1 and Q_2 states can contr bute to the approximately 4 Cv of kinetic energy released to the pair of' excited Ii--atoms at the peak of t h e 3p kinetic energy distribution in Fig. 3. However, The Q_1 state is the source of fas(H-atoms between 23 and 30 CV impact energies.[4,5] The 1owcsI Q_1 ($^1\Sigma_g^+(1)(2p\sigma_u)^2$) state crosses the Franck-Condon region at 23 cV. in our case, a curve crossing of this doubly excited state via homogeneous perturbation with the dissociating state ($1s\sigma_g)(3\ell)$ (16.67cV dissociating energy) leads to the first group of fast H-atoms for n=3.

Ogawa and co-workers have carefully measure.d the central peak of the Hα line profile. They find the central peak of the Hα line profile to have a FWHM of 0.32Å at 100 CV impact energy. They also find the central peak to be asymmetric duc to fine structure. They find the same results as illustrated here from the point of view of line profile and kinetic energy distribution in Fig. 2 and Fig. 3, respectively, for the ratio of the fast to slow component H-atom intensities. The relative intensity of fast atoms increases with increasing principal quantum number. For H=2p we found that 31% of the atoms released in the dissociation processes arc fast.[4,5] Integrating under the kinetic energy distribution curve for H=3p in fig. 3, wc find that 47 % of the atoms expelled in the dissociation process arc fast. on ι qualitative basis the line profile. compariso IS in Fig. 2 show the same resu ts. If wc take the central core FWHM repor ed by Ito ct al. [1] and divide by six, we would predict that the H Lβ central core should be **50** mÅ FWHM. On the other hand, our results suggest a FWHM of less than 30 mÅ. The difference may be ascribed to the lack of resolution in the Hα measurements to separate all the fine structure components. The complex line at 6562.8Å is composed of three multiplets at 6562.86 (2p-3s), 6562.74 (2s-3p) and 6562.81 (2p-3d). Under higher resolution there are seven lines. The maximum separation is 120 mÅ and shows the difficulty of determining the slow atom energy (distribution from Hα line profiles.

DISCUSSION

We have measured the line profile of H Lβ for the first time, and compared it to. a higher resolution line profile of H Lα. The resolution was sufficient to determine the kinetic energy distribution function of fast H(3p) atoms from an analysis of the blue wing at 100 eV impact energy. Accurate analysis of the slow energy peak requires higher resolution studies of the line central peak. Preliminary results from our measurement indicate a line FWHM of less than 30 mÅ and a kinetic energy distribution with peak energy between O and 1 eV. The quantum yield of fast and slow atoms released in the various types of dissociation processes is 0.53 for slow atoms and 0.47 for fast atoms. A comparison of the fast kinetic energy distribution for H(3p) from this experiment to that of H(3s,3p,3d) of Ogawa and co-workers arc very similar. This result suggests that the three 1 lα multiplets have the same line profile at 100 CV electron impact energy.

Our direct measurement of the 11 Lβ cross section at 100 CV electron impact energy by two different methods arc in very good agreement with onc another and yield an absolute cross section of 3.28 ± 0.80 x 10-19 cm^2. Duc to blending with nearby L & W bands, this measurement required a n estimate of the profile of the red wing. We assumed the line profile was symmetric, which causes about 10% uncertainty in the cross section. W c can extend tbc absolute cross section result at 100 CV to other energies b y normalizing the low resolution Hα cross section results of Karolis a n d Harting[7] from 0-105 CV and of Freund et al.[16] beyond 100 cV. This result is shown in Fig. 4. The excitation function indicates the four thresholds found by Karolis and Harting at 16, 26, 35 and 43 eV. Recently from high resolution studies of the excitation function of the Hα wing, Ogawa et al.[3] found thresholds at **22-23** and **27** eV. in addition, wc show in Fig. 4 the cross section for the entire blended feature of Fig. 1, inducting H Lβ and L & W features of Table 1. The cross section of the blended feature is 5.69 ±

0.80 x 10^{-19} cm^2 at 100 eV. The peak cross section for both excitation functions in Fig. 4 occur near 80 eV.

our previous indirect estimate of the HLβ cress section of 8.3 x 10^{-19} cm^2 at 100 CV was based on the 3s, 3p, 3d excitation rates of Julien et al.[21] and Glass-Maujean[22] However, the excitation rates were measured at threshold (near 16.56 eV) and may change at higher energy. Additionally, these authors have measured the velocity distribution]] of fast and slow atoms, using measurements of anti-crossing signals between Zeeman sub-levels. They have detected slow atoms with energies between 0.3 to 0.4 eV and fast atoms with energies of - 10 eV in good agreement with the results for fast atoms presented here. The Doppler shift[21,22] for the slow atoms corresponds to -30 mÅ, also in excellent agreement with our estimate.

Wc can also make an estimate of the contribution of 3p atoms to the Hα cross section. The branching ratio, ω_{1s3p}, for is-3p emission is 0.881. The excitation cross section for 3p at 100 CV can be found to be $Q_{l\beta}/\omega_{1s3p}$=3.72 X 10^{-19} cm^2. On this basis wc estimate that the 3p atoms contribute 40.0 ± 10% of the total Hα cross section of 9.3 x 10^{-19} cm^2.[7] This fractional percentage indicate there is probably no preferential population of 3s, 3p, 3d sub-levels and the Hα radiation is nearly the sum of the cross sections for 11(3s) and H(3d) dissociation. At 100 cV. Our results indicate that the contribution to Hα is 4.7% in agreement with earlier conclusions by Vroom and de Heer.[23] Vroom and de Heer also indicate an upper limit to H(3p) dissociative cross section of 3.57 x 10^{-19} cm^2 at 50 eV. The cross section plot in Fig. 4 can be used to give the H(3p) cross section of 3.18 x 10-19 cm^2 at **50 Cv.**

ACKNOWLEDGMENTS

The research described in this text was carried out at the Jet l'repulsion laboratory, California Institute of Technology. The work was supported by the Air Force Office of Scientific Research (AFOSR), the Aeronomy Program of the National Science Program (grant ATM-9320589 to the University of Southern California) and NASA Planetary Atmospheres, Astronomy/Astrophysics and Space Physics Program Offices. S. M. Ahmed and X. Liu are supported by a National Research Council Resident Research Associateship.

REFERENCES

[1] K. Ito, N. Oda, Y. Hatano and T. Tsuboi, Chem. Phys. **17**, 35 (1976).

[2] M. Higo, S. Kamata and 1. Ogawa, Chem. Phys. **73**, 99 (1982).

[3] 'I'. Ogawa, Y. Jinbou, N. Yonekura, K. Furuya, K. Nakashima, Bull. Chem Sot. Japan, **66**, 3506 (1993).

[4] J. M. Ajello, S. M. Ahmed, 1. Kanik anti R. Multari, Phys. Rev. Lett. In Submission (1995).

[5] J. M. Ajello, I. Kanik, S. M. Ahmed and J. T. Clarke, J. Geophys. Res. In I'less (1 995).

" X. Liu, S. M. Ahmed, R. A. Multari, G. K. James and J. M. Ajello, Ap. J. Sup. InPress (1995).

[7] C. Karolis and E. Harting, J. Phys. B, **11**, 357 (1978).

[8] J. M. Ajello, D. Shemansky, T. L. Kwok, Y. L. Yung, Phys. Rev. A, 29, 63 6 (1984).

[9] Clarke, J. T., L. Ben Jaffel, A. Vidal-Madjar, G. R. Gladstone, J. H. Waite, R. Prange, J. Gerard, J. Ajello and G. James,] , Ap. J. Lett. 430, 1.73-1.76, 1994.

[10] Clarke, J. T., G. R. Gladstone, and L. Ben Jaffel, Geophys. Res. Lett. **18**, 1935, 1991.

" J. M. Ajello et al. Appl. Opt. **27**, 890 (1988)

[12] 11. Abgrall, E. Roueff, F. Launay, J.-Y. Roncin and J.-L. Subtil, J. Molec. Spectrosc. 157, 512 (1993a).

[13] H. Abgrall, E. Roueff, F. Launay, J.-Y. Roncin and J.-L. Subtil, Astron. Astro. *101,* 2'73 (1993 b).

[14] H. Abgrall, E. Roueff, F. Launay, J.-Y. Roncin and J.-L. Subtil, Astron. Astro. **101**, 323 (1993 c).

[15] Press, W. H., B. P. Flannery, S. A. Teukolsky and W. T. Vettering, *Numerical Recipes* (Cambridge University Press, Cambridge, England, 1987

[16] R. S. Freund, J. A. Schiavone and D. F. Brader, J. Chem. Phys. 64, 1122 (1976).

[17] S. R. Ryan, J. J. Spezeski, O. F. Kalmam, W. E. Iamb, L. C. McIntyre, and W. 11. Wing, Phys. Rev. A, 19, 2192 (1979).

[18] J. M. Ajello D. E. Shemansky and G. K. James, Ap. J. 371, 422 (1991).

[19] T. Ogawa and M. Higo, Chem. Phys. Lett. 65, 610 (1 979).

[20] S. 1.. Guberman, J. Chem. Phys. 78, 1404 !983).

[21] L. Julien, M. Glass-Maujean and J. P. Descoubes, J. Phys. B, 6, 1.196 (1973).

22 M. Glass-Maujean, J. Phys. B, **11**, 431 **(1978).**

2.1). A. Vroom and F. J. de Heer, J. Chem. Phys. **50**, 580 (1969).

Table 1 H_2 Emission Spectral Intensities near H Lyman-β Transition

Wavelength (Å)	Intensity[1]	Relative Intensity	Assignment[2]
1025.880	3.0490E-02	2.1256E-03	2(10, 5) P Werner
1025.886	4.6709E+00	3.2563E-01	1 (5, 3) Q Werner
1025.888	8.6408E-19	6.0240E-20	13(13, O) R Lyman
1025.895	2.3861E-04	1.6635E-05	4(11,11) Q D
1025.911	1.4344E+01	1.0000E+00	1(3, 2) Q Werner
1025.918	8.3739E-08	5.8379E-09	8(2, 5) QD
1025.922	1.0748E-07	7.4930E-09	6(11, 5) R Werner
1025.935	7.3617E+00	5.1323E-01	1 (6, O) P Lyman
1025.936	6.8840E-03	4.7992E-04	3(10, 5) R Werner
1025.957	5.9106E-O2	4.1206E-03	3 24, 4) P Lyman
1025.961	5.1620E-08	3.5987E-09	8 4, 2) Q Werner
1025.974	4.3545E-09	3.0358E-10	1 36, 5) P Lyman
1025.998	5.8953E-05	4.1099E-O6	6 5, 5) R B'
1026.016	2.2821E-10	1.5910E-11	1 35, 5) R Lyman
1026.019	8.7148E-02	6.0756E-03	1 14, 2) P Lyman
1026.072	1.3969E-13	9.7386E-15	10(19, 2) R Lyman
1026.079	3.51OOE-OI	2.4470E-02	3(3, 6) Q D
1026.096	5.1721E-05	3.6058E-06	3(16,14) Q D
10?6.099	5.1928E-09	3.6202E-10	10(1, 3) P B'

1 Effective intensities (unit: 10^{-20} photon per H_2 molecule)

2 Transition is labelled by J"(v', v") ΔJ. Lyman, Werner, B', and D refer to 2pσ $B\,^1\Sigma_u^+ \leftrightarrow X\,^1\Sigma_g^+$, 2pπ $C\,^1\Pi_u \leftrightarrow X\,^1\Sigma_g^+$, 3pσ $B'\,^1\Sigma_u^+ \leftrightarrow X\,^1\Sigma_g^+$, and 3pπ $D\,^1\Pi_u \leftrightarrow X\,^1\Sigma_g^+$ electronic transitions, respectively.

TABLE OF FIGURES

FIGURE 1. Overplot of experimental spectra: a) 100 eV H Lβ line profile in second order (open diamonds); b) 100 eV H Lα line profile in third order (filled squares) ; c) zero order slit function of experimental apparatus scaled to second order (plus signs). The data statistics were better than 1% in a), b) and c).. The wavelength step size in second order was 4 mÅ and in third order was 2.667 mÅ. The operating conditions were established as follows: 1) background gas pressure of 2.3×10^{-4} torr and 2) electron beam current of 130 A. Peak signal was 4000 and 13000 counts in the 100 eV H Lβ and H Lα line profiles ,respectively, with background signals of under 100 counts.

FIGURE **2.** Deconvolution of the 100 eV line profiles data of H Lβ (solid line) and H Lα (dash line) of Fig. 1 along with a comparison to published data of Hα line profiles.

FIGURE 3. Fast H(3p) and H(2p) atom kinetic energy distribution functions.

FIGURE 4. Estimated absolute cross section of H Lβ from published optical excitation function measurement of Hα. The excitation function measurements of Karolis and Harting[7] **shown** as open diamonds from 0 - 100 CV and Freund et al.[16] shown as plus signs from 100- 290 cV, arc normalized to the 100 CV cross section of H Lβ from this work. The cross section of the blended }1 Lβ & and 1. & W feature from this work is shown as a filled square.

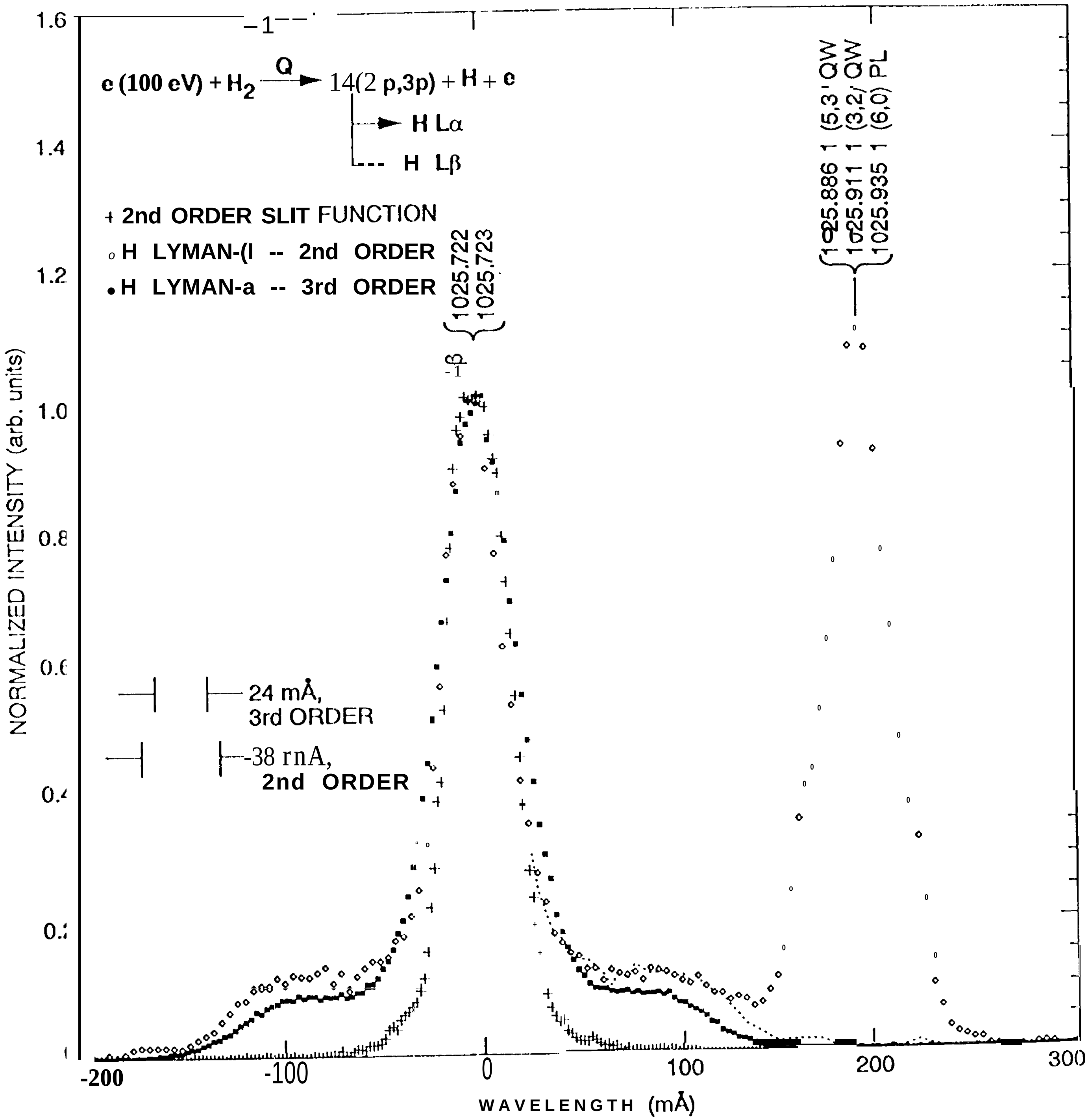

e (100 eV) + H_2 Q 14(2 p,3p) + H + e
H Lα
H Lβ
+ 2nd ORDER SLIT FUNCTION
o H LYMAN-(I -- 2nd ORDER
• H LYMAN-a -- 3rd ORDER
1025.722
1025.723
1025.886 1 (5,3') QW
1025.911 1 (3,2) QW
1025.935 1 (6,0) PL
24 mÅ, 3rd ORDER
38 mÅ, 2nd ORDER
NORMALIZED INTENSITY (arb. units)
WAVELENGTH (mÅ)

Fig. 1

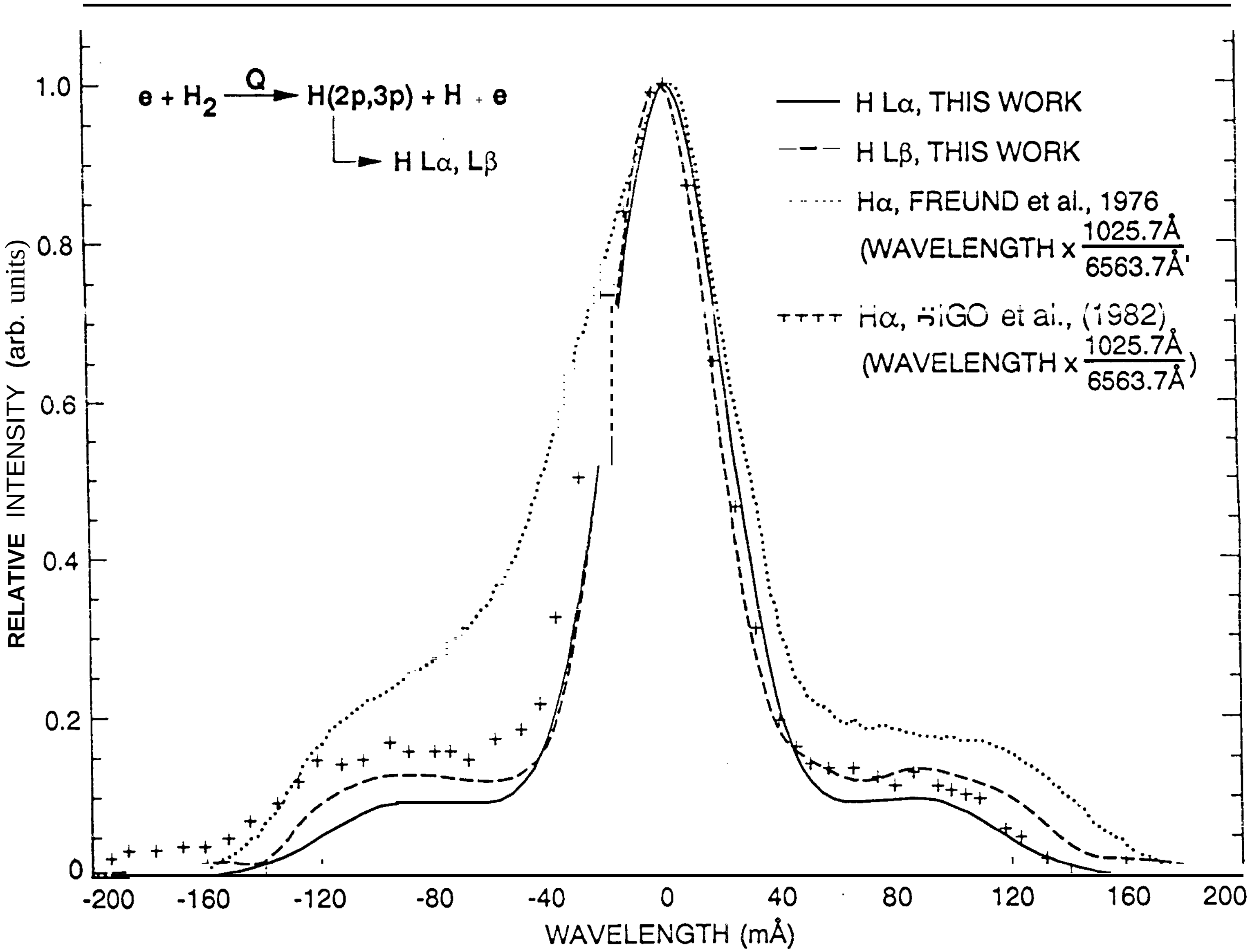

e + H2 Q H(2p,3p) + H + e
H Lα, Lβ
H Lα, THIS WORK
H Lβ, THIS WORK
Hα, FREUND et al., 1976
(WAVELENGTH x 1025.7Å / 6563.7Å)
Hα, HIGO et al., (1982)
(WAVELENGTH x 1025.7Å / 6563.7Å)
RELATIVE INTENSITY (arb. units)
0
0.2
0.4
0.6
0.8
1.0
-200
-160
-120
-80
-40
0
40
80
120
160
200
WAVELENGTH (mÅ)

Fig 2

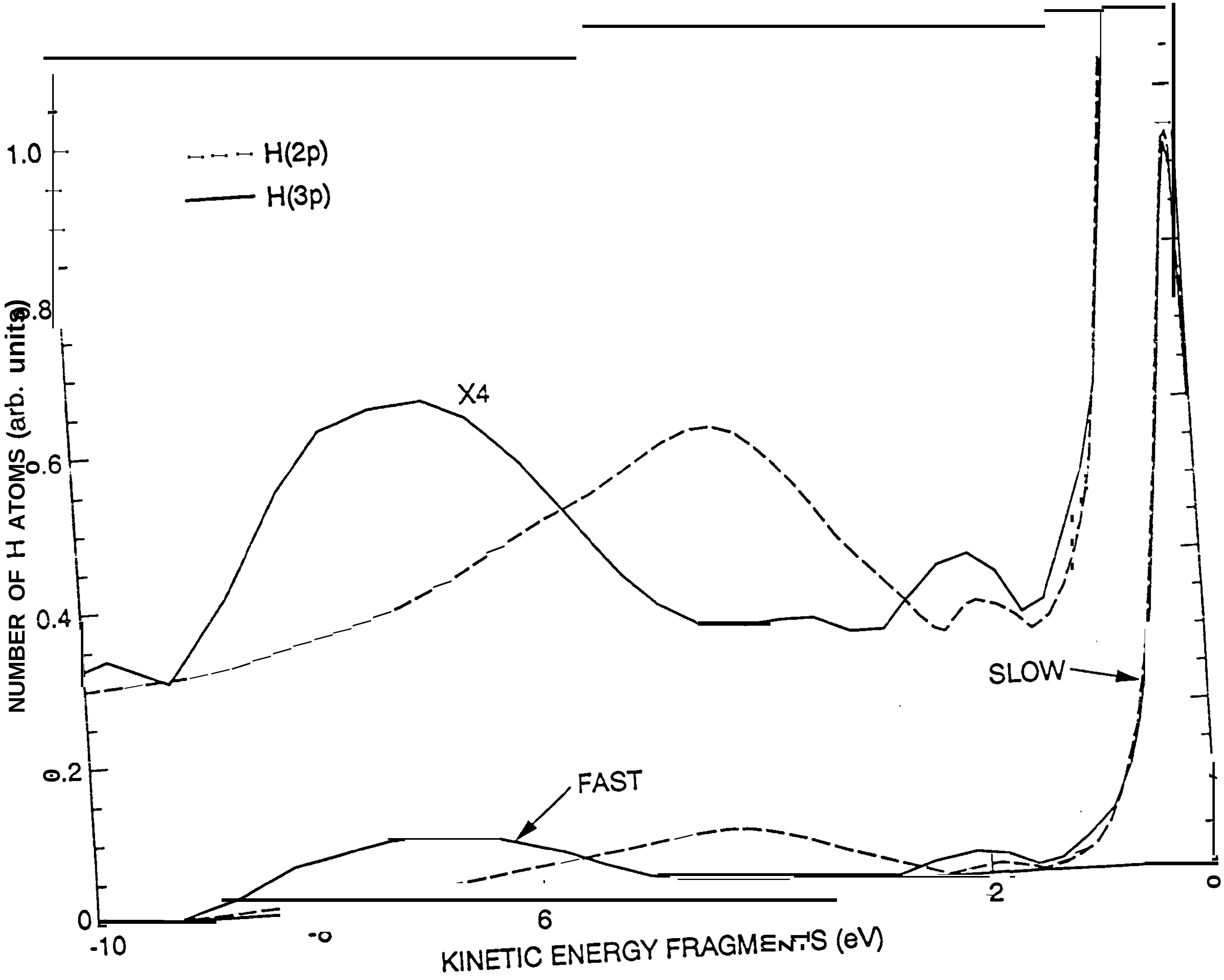

NUMBER OF H ATOMS (arb. units)
1.0
0.8
0.6
0.4
0.2
0
H(2p)
H(3p)
X4
SLOW
FAST
-10
6
2
0
KINETIC ENERGY FRAGMENTS (eV)

Fig. 3

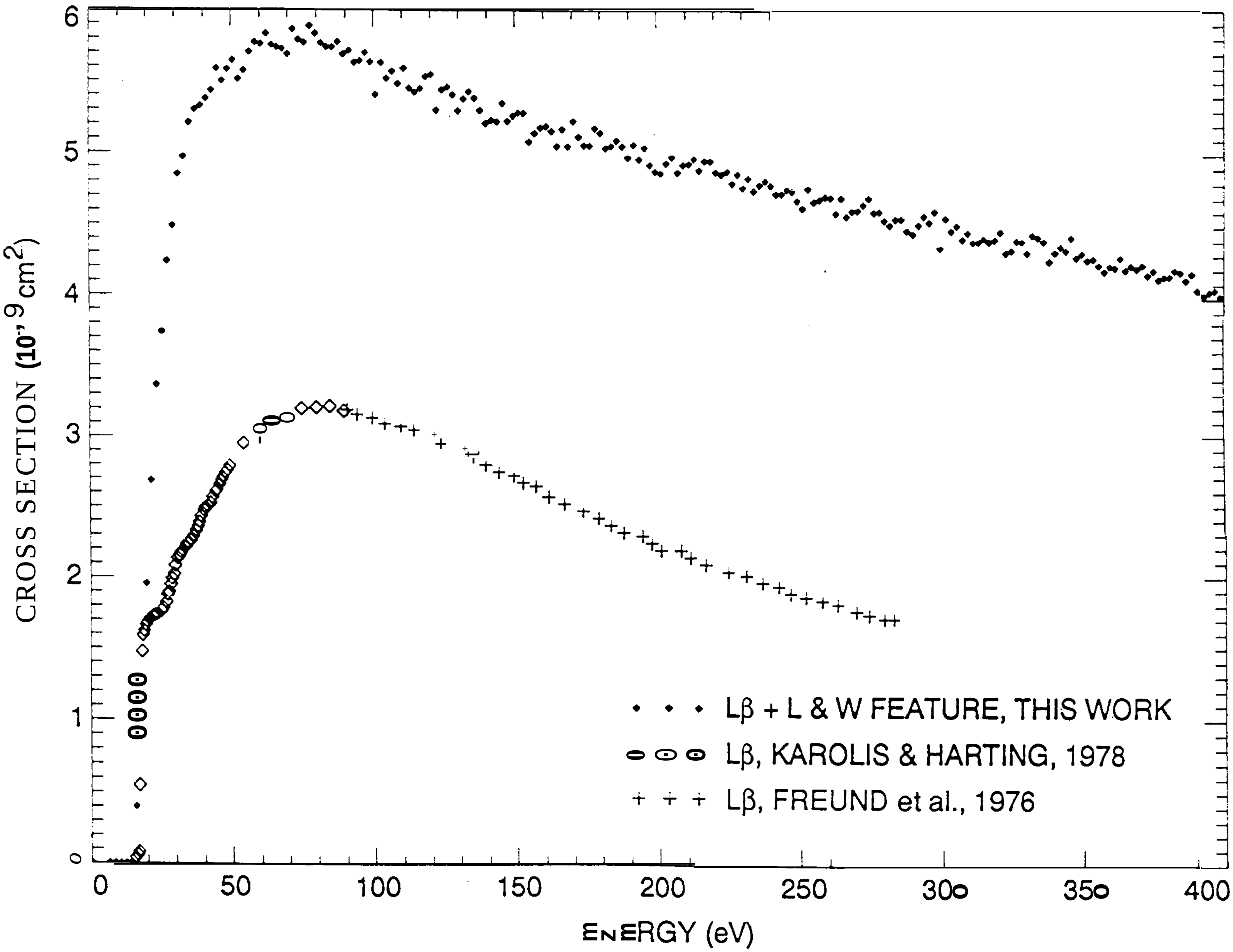
CROSS SECTION (10^{-19} cm^2)
0
1
2
3
4
5
6
0
50
100
150
200
250
300
350
400
ENERGY (eV)
Lβ + L & W FEATURE, THIS WORK
Lβ, KAROLIS & HARTING, 1978
Lβ, FREUND et al., 1976

Fig 4